A&A 379, 616–621 (2001)
DOI: 10.1051/0004-6361:20011342

Astronomy & Astrophysics

The timing of non-thermal soft X-ray emission line broadenings in solar flares

N. D. R. Ranns, L. K. Harra, S. A. Matthews, and J. L. Culhane

Mullard Space Science Laboratory, University College London, Holmbury St. Mary, Dorking, Surrey, RH5 6NT, UK

Received 19 October 2000 / Accepted 24 September 2001

Abstract. We study 59 solar limb flares using the Bragg Crystal Spectrometer (BCS) on Yohkoh and the Burst and Transient Source Experiment (BATSE) to investigate the relative timings between the Hard X-Ray (HXR) emission and the observed non-thermal broadenings of X-ray emission lines ($V_{\rm nt}$). We show that the duration of the HXR flux rise to maximum emission affects the relative timing of the main $V_{\rm nt}$ peak with respect to the main HXR peak. In ≈20% of the flares studied, secondary peaks in $V_{\rm nt}$ are observed. These are always associated with a strong HXR pulse and usually occur after the associated HXR pulse. There are also flares that show a relationship between the decay times of $V_{\rm nt}$ and HXR flux. These results are conducive to a causal relationship between the HXR flux and $V_{\rm nt}$. We divided the sample of flares into two classes, gradual rise and impulsive rise, depending on the shape of the HXR lightcurve up to maximum emission. We show that the $V_{\rm nt}$ behaviour differs in the two classes. The implications are discussed with a view to understanding the mechanism of $V_{\rm nt}$ generation.

Key words. Sun: flares – Sun: general – Sun: X-rays, gamma rays

1. Introduction

During the early phases of a solar flare the level of SXR non-thermal line broadening is greatly enhanced over background levels. The non-thermal broadening is defined as the difference between the Doppler temperature ($T_{\rm d}$) and the plasma temperature ($T_{\rm e}$). In an ionized He-like species these temperatures are derived from the width of the main resonance line and the ratio of the main resonance line and the satellite lines respectively. This temperature difference is often expressed as a non-thermal velocity ($V_{\rm nt}$) where;

$$V_{\rm nt} = \sqrt{\frac{2k(T_{\rm d} - T_{\rm e})}{m_{\rm i}}}, \quad (1)$$

where k is the Boltzmann constant and $m_{\rm i}$ the mass of the ion under consideration.

The study of $V_{\rm nt}$ in solar flares is important as it may be related to the flare energy release process (Tsuneta 1994, 1995; Alexander et al. 1998). Previous studies of the timing relationships between $V_{\rm nt}$ and HXRs (Alexander et al. 1998; Mariska & McTiernan 1999) showed that the $V_{\rm nt}$ peaks early in the HXR burst often before the HXR maximum flux but after the first significant HXR peak. Such behaviour is consistent with the $V_{\rm nt}$ being related to the initial energy release process rather than a hydrodynamic response of the electron deposition (Alexander et al. 1998). Alexander et al. (1998) also note that the decay phase of $V_{\rm nt}$ displays no strong signature of subsequent individual HXR bursts.

Attempts to locate the source of the $V_{\rm nt}$ within a flare structure (Khan et al. 1995; Mariska & McTiernan 1999; Ranns et al. 2000) have eliminated the flare footpoints as possible source locations and indicated that the source is within or above the flare loops. However, these studies could not differentiate between the source of $V_{\rm nt}$ as either evaporating chromospheric plasma or plasma that is related to the initial flare energy release, since both possibilities were consistent with the results.

In the model for $V_{\rm nt}$ generation in a turbulent evaporation flow we assume that the magnitude of $V_{\rm nt}$ is directly linked to the amount of electron energy converted to evaporation. Therefore large inputs of electron energy to the chromosphere, signalled by a HXR peak should be followed by a $V_{\rm nt}$ peak. However if the $V_{\rm nt}$ is generated by plasma associated with the initial energy release, then the $V_{\rm nt}$ peak would be expected to precede or be coincident with the HXR peaks. The model of Tsuneta (1994, 1995) is an example of such a model. Turbulent plasma above the loop top is generated by the collision of the reconnection jet. The time varying turbulence subsequently accelerates the electrons that produce the HXR burst. It should, therefore, be possible in the simplest scenario to

Send offprint requests to: S. A. Matthews,
e-mail: sam@mssl.ucl.ac.uk

distinguish between these two models based purely on the timing relationships between $V_{\rm nt}$ and HXR flux. This is attempted in this study.

In this study we examine 59 solar flares that occurred on the limb and were observed simultaneously by BATSE and BCS. All these flares displayed a discernible peak in the observed $V_{\rm nt}$ measured by BCS. In Sect. 2 we describe these two instruments and outline the flare selection process. We analyse these flares in Sect. 3 and show that a relationship exists between the HXR rise time and the time delay between the $V_{\rm nt}$ and HXR peak times. In Sect. 4 we discuss the implications of our results.

2. Observations and instrumentation

This study uses data taken with the *Burst And Transient Source Experiment* (BATSE) on-board the *Compton Gamma Ray Observatory* (CGRO) and the *Bragg Crystal Spectrometer* (BCS) on-board *Yohkoh*. BCS is a full Sun spectrometer that uses four bent crystals to observe the Sun in four discrete wavelength ranges. These ranges cover the principle emission lines of He-like S XV, Ca XIX and Fe XXV and H-like Fe XXVI (Culhane et al. 1991).

BATSE is a whole sky HXR flux monitor that consists of eight identical uncollimated Large Area Detector (LAD) modules situated at the faces of an octahedron that is formed by the three major axes of *CGRO*. The LADs, sensitive to photons in the range 25 → 2000 keV range, are Na I scintillation crystals with a geometric area of 2025 cm^2, which yield an angular response that is proportional to $\cos\theta$ at energies less than 300 keV. The energy resolution of the LADs is ≈27% at 88 keV and increases with energy (Fishman et al. 1989)

To obtain the dataset used in this analysis we automatically searched the BATSE solar flare data base, from *Yohkoh* launch (30th August 1991) to CGRO decommissioning (4th June 2000), for all events that exceeded a peak count rate of 500 counts per second in BATSE's low energy channel (25 → 50 keV). Flares with a count rate greater than this threshold appeared to have a correspondingly good signal in the BCS Ca XIX channel. The resulting flares were then included into a preliminary data set if they

a) Occurred at angle greater than 60° from Sun centre. This criterion was set in an attempt to exclude any blue-shifted plasma components in the line profiles;
b) Occurred during *Yohkoh* day and not during an SAA passage by the satellite.

For all the flares matching the above criteria the corresponding spectral data from the BCS Ca XIX channel were fitted using the standard BCS software. The fitting procedure generates theoretical spectra which are fitted to the data via χ^2 minimization. The resulting fitted data were then examined manually for flares that showed a well defined peak in $V_{\rm nt}$. Any events in which a blue-shifted component was present were discarded. Due to the orientation of the Bragg crystal in the BCS, the wavelength dispersion axis is aligned with solar longitude. Therefore emission lines from sources at different latitudes appear at different wavelengths in the BCS detector. If two sources were determined to be present during the early stages of a flare, then it was discarded. This procedure yielded 59 events for further analysis.

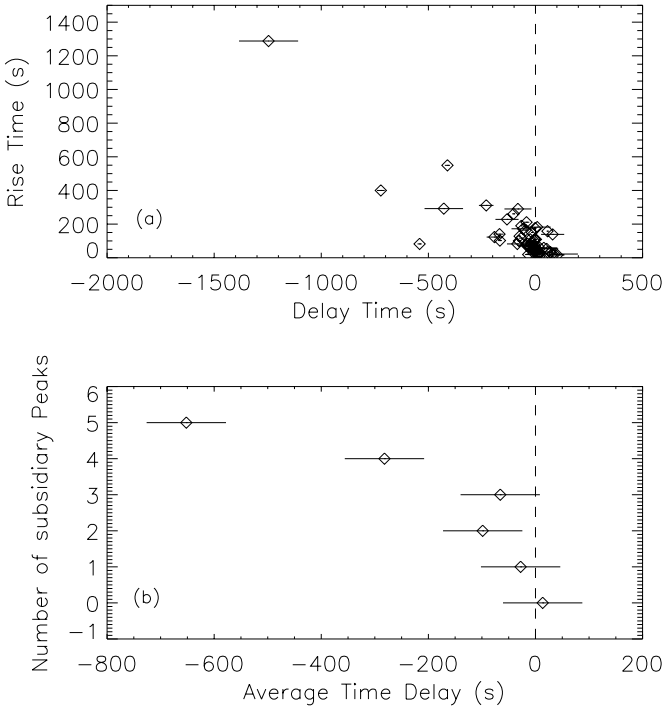

Fig. 1. a) The relationship between the HXR rise time and the delay time between the HXR maximum and $V_{\rm nt}$ maximum, **b)** the average time delay for flares with a particular number of subsidiary peaks. A negative delay time implies that the $V_{\rm nt}$ peak occurred before the HXR peak.

3. Analysis

In the absence of any other a priori information on the plasma state, when analysing BCS data, we must assume that the plasma is isothermal. From the flare spectrum we then obtain $T_{\rm e}$, $T_{\rm d}$ and consequently $V_{\rm nt}$ of the whole flare. From all the flares studied we calculated the following parameters:

a) time and magnitude of the main $V_{\rm nt}$ peak;
b) time and magnitude of the main HXR peak;
c) the start time and rise time of the HXR emission.

The start time of the HXR emission was defined as the time at which the flux exceeded 3σ above the pre-flare background level and the rise time was defined as the time elapsed from the HXR start time to time of maximum emission.

Figure 1a shows a plot of the HXR rise time ($t_{\rm rise}$) versus the time delay between the HXR flux peak and the $V_{\rm nt}$ peak ($t_{\rm delay}$). A negative $t_{\rm delay}$ implies that the $V_{\rm nt}$ peak occurred before the HXR peak. From the whole data set, 22 flares had a positive time delay and 37 a

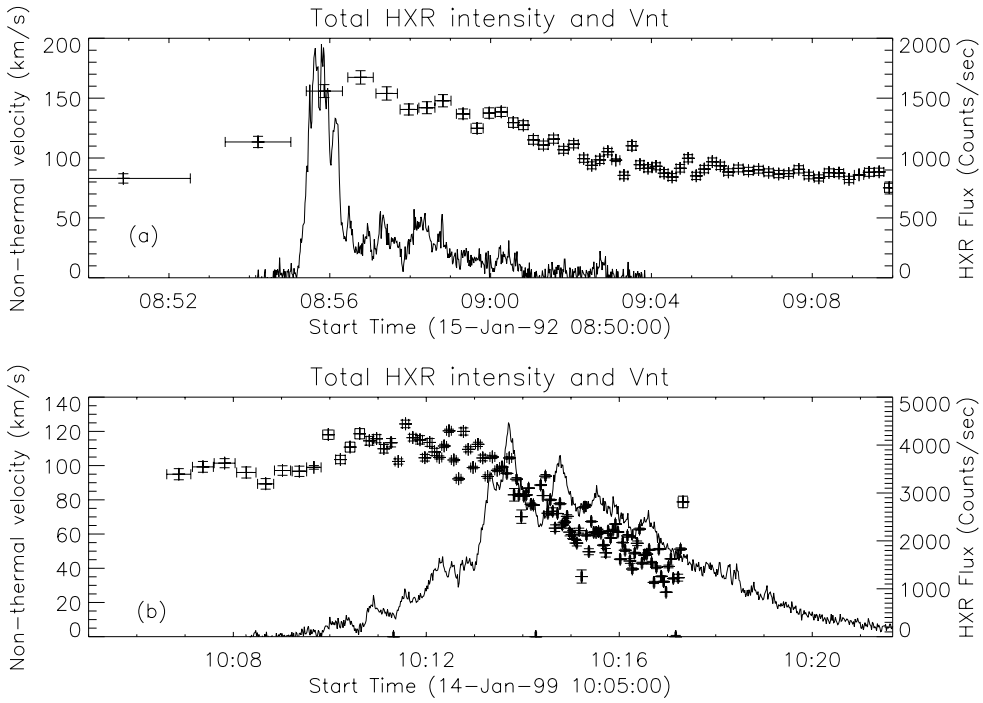

Fig. 2. Graphs showing $V_{\rm nt}$ (with error bars) and HXR flux for two flares in the dataset. **a)** An example of an impulsive rise HXR burst and **b)** an example of a gradual rise HXR burst.

negative time delay. The greater number of negative delay flares is in agreement with the results of Alexander et al. (1998). However, this may result from selection effects. Some flares that were originally examined for inclusion into the final data set had short HXR rise times but no BCS spectra were obtainable before the HXR peak, hence these events were not included in the dataset because no discernible $V_{\rm nt}$ peak was observed.

In the introduction we described how the turbulent evaporation flow model should show $V_{\rm nt}$ peaks after HXR peaks, whereas models invoking turbulent plasma associated with the initial energy release should display $V_{\rm nt}$ peaks before HXR peaks. In this sample both cases are observed, suggesting that there may be two classes of flares that are consistent with both scenarios.

However Fig. 1a shows that $t_{\rm rise}$ and $t_{\rm delay}$ are related. A longer HXR rise time implies a greater time delay between the $V_{\rm nt}$ and HXR peaks. In the models of $V_{\rm nt}$ generation outlined in the introduction the HXR flux and $V_{\rm nt}$ are proposed to correlate in time with a possible time lag, neither model predicts the variation of $V_{\rm nt}$ peak timing with the duration of the HXR burst. Therefore other factors must also be present that influence the timing of the $V_{\rm nt}$ peak. We will discuss these in Sect. 4. Figure 1b shows how the average $t_{\rm delay}$ varies for flares with a particular number of subsidiary HXR bursts that occur before the main HXR peak. The greater the number of subsidiary peaks the earlier the $V_{\rm nt}$ peak occurs before the HXR peak.

To further investigate the relationship between $t_{\rm rise}$ and $t_{\rm delay}$ we separate our sample of flares into two categories: *impulsive rise flares* and *gradual rise flares*. An *impulsive rise flare* has a HXR profile that has a sharp rise to maximum emission in a single smooth peak, an example is shown in Fig. 2a. A *gradual rise flare* has a slow rise to maximum with one or more subsidiary peaks (Fig. 2b). Historically flares with gradual HXR emission are more commonly related to long duration events (LDEs) and two ribbon flares, whereas flares that display impulsive HXR lightcurves are often related to compact flares (Bai & Sturrock 1989).

Histograms of the measured parameters for these flares are shown in Fig. 3 for both *impulsive rise flares* and *gradual rise flares*. The total number of *Gradual Rise Flares* is 35 and *Impulsive Rise Flares* 24. The histograms show a clear tendency for *Impulsive Rise Flares* to have a shorter delay time than the *Gradual Rise Flares*. The shorter rise time of the *Impulsive Rise Flares* is also evident. No distinction between *Gradual Rise Flares* and *Impulsive Rise Flares* is evident from maximum HXR flux, however there is a possible tendency for *Impulsive Rise Flares* to exhibit a larger maximum $V_{\rm nt}$. In *Impulsive Rise Flares* the $V_{\rm nt}$ peak occurs after the main HXR peak in 66% of events. In *Gradual Rise Flares* the $V_{\rm nt}$ peak occurs after the main HXR peak in 25% of events. Ideally we would also provide results on the measured rise times of $V_{\rm nt}$. However, as can be seen from Figs. 2, 4 and 5 there are few cases where we have reliable measurements of $V_{\rm nt}$ for the whole of the rise phase. In order to minimize the possibility of spectral contamination from other active regions we used Ca XIX which is formed in the range $\log T_{\rm max} = 7.1 \rightarrow 7.2$. Hence, extended pre-flare emission in this line complex is rare. Information on the rise time of $V_{\rm nt}$ may have

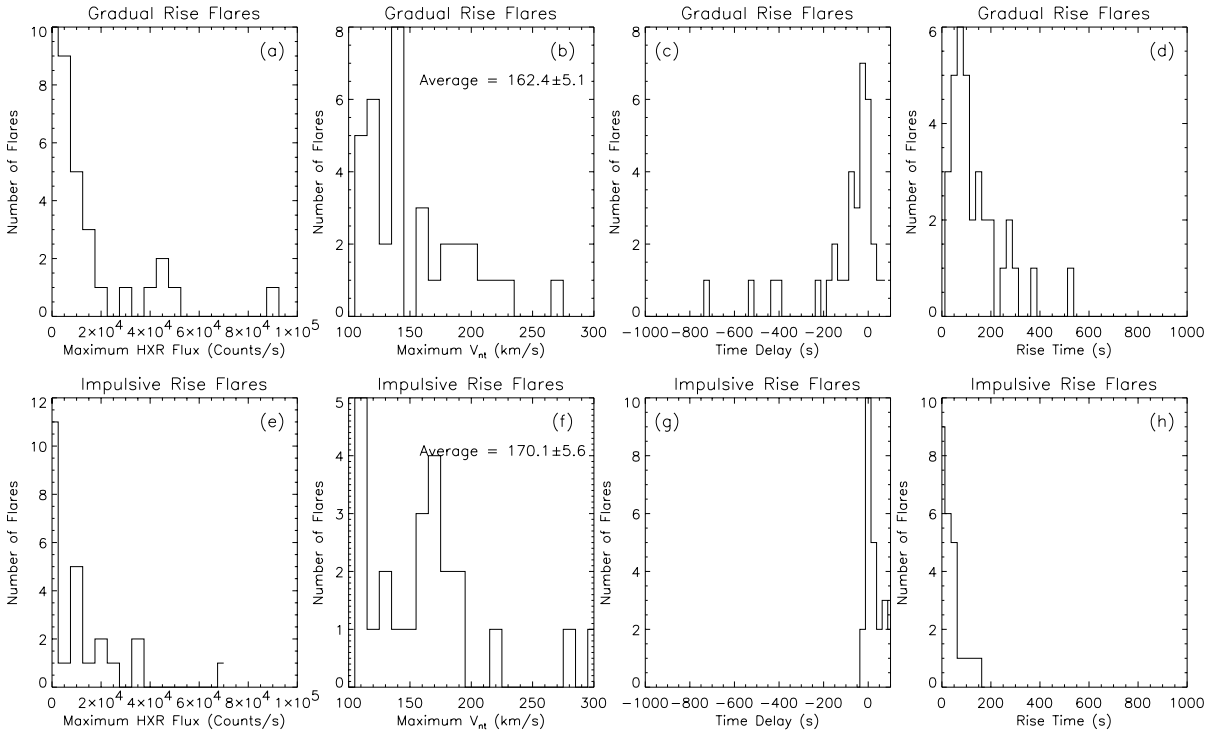

Fig. 3. Histograms of maximum HXR flux (**a)** and **e)**), maximum $V_{\rm nt}$ (**b)** and **f)**), delay time (**e)** and **g)**) and rise time (**d)** and **h)**) for *Impulsive Rise Flares* (**a)**, **b)**, **c)**, and **d)**) and *Gradual Rise Flares* (**e)**, **f)**, **g)**, and **h)**).

indicated whether it varied independently of the HXR emission. However, it is still clear from these results that there are systematic differences in the behaviour of $V_{\rm nt}$ in impulsive and gradual rise flares.

Figure 4 shows $V_{\rm nt}$, HXR and BCS count rates for two flares in the data set. These two examples clearly show that when a large HXR pulse occurs $V_{\rm nt}$ also increases. This type of behaviour occurred in only ≈20% of the studied flares of which 75% were *Gradual Rise Flares*. We note that in the examples in Fig. 4 the strong HXR peak and corresponding $V_{\rm nt}$ peak occur at times when the BCS count rate is increasing but still at low values.

Figure 5 shows $V_{\rm nt}$ and HXR flux for two flares in the data set. These two examples show that there is a possible relationship between the decay time of $V_{\rm nt}$ and the decay time of the HXR flux. The longer the HXR burst lasts after attaining maximum flux, the longer the enhanced levels of $V_{\rm nt}$ are present. This relationship does not hold for all flares (e.g. Fig. 4b) due to the effects of line narrowing. Line narrowing is an instrumental effect that artificially narrows the main resonance line in BCS data. This effect is most significant when the count rate is high (Trow et al. 1994).

4. Discussion

The main observational results from this study are listed below.

a) i) There exists a relationship between the HXR rise time ($t_{\rm rise}$) and the time delay between the $V_{\rm nt}$ and HXR peak ($t_{\rm delay}$).
   ii) $t_{\rm delay}$ is also related to the number of subsidiary HXR peaks that occur before the main HXR peak.
b) Approximately 20% of flares studied showed secondary peaks in $V_{\rm nt}$ that were always associated with HXR peaks. Secondary peaks occur after the HXR peak.
c) A possible relationship exists between the decay times of $V_{\rm nt}$ and HXR flux.
d) There are systematic differences in the $V_{\rm nt}$ behaviour in impulsive rise and gradual rise flares. Gradual rise flares show a tendency for $V_{\rm nt}$ to peak before the HXR peak, whereas the opposite behaviour is observed in impulsive rise flares.

The relationship between $t_{\rm rise}$ and $t_{\rm delay}$ supports the argument for a link between the HXR flux and $V_{\rm nt}$ because it implies that the HXR flux before the HXR peak is influential in determining the time of the $V_{\rm nt}$ peak. In addition to this general trend there are examples of direct responses of $V_{\rm nt}$ to a large HXR pulse and flares that suggests that the longer HXR flux persists the longer the elevated levels of $V_{\rm nt}$ are observed. These examples also support the existence of a causal relationship between the HXR flux and $V_{\rm nt}$.

We stated in the introduction that the two mechanisms for $V_{\rm nt}$ generation, i.e. turbulent evaporation flow and loop top turbulence associated with the initial

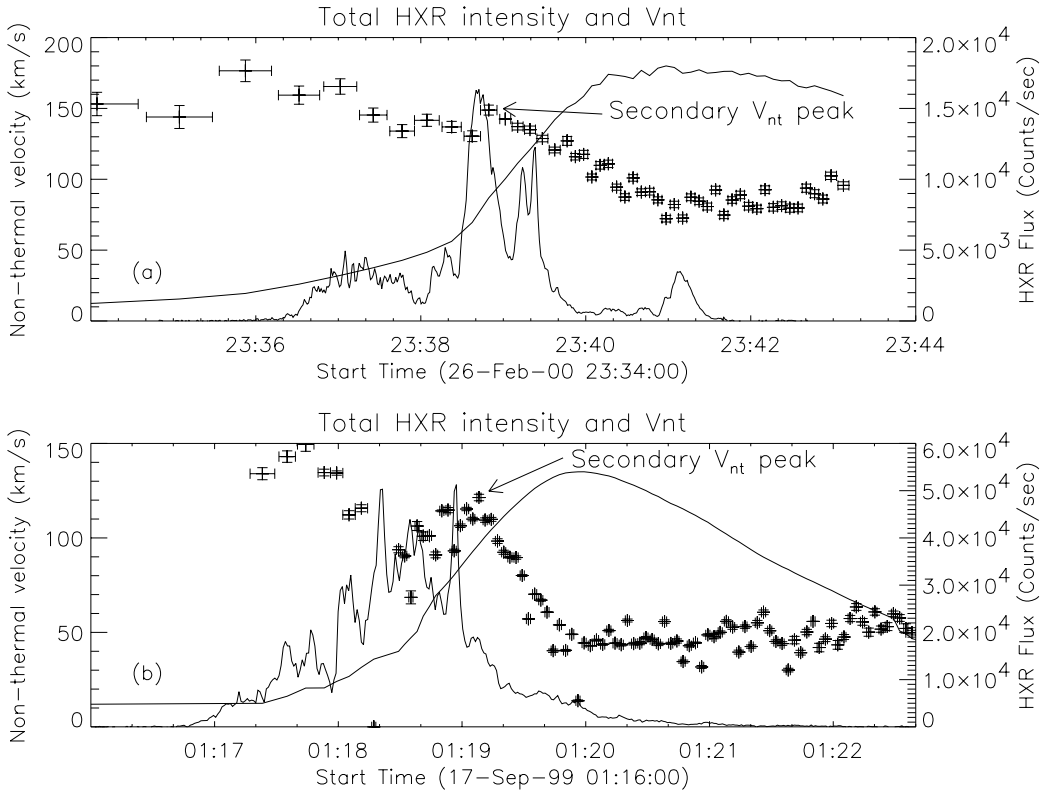

Fig. 4. Graphs showing $V_{\rm nt}$ (with error bars), HXR flux and BCS count rates (arbitrary scale). These are two clear examples of $V_{\rm nt}$ increases at times of strong HXR pulses.

energy release, could be separated based on the timing relationships between $V_{\rm nt}$ and HXR peaks. The turbulent evaporation model will produce $V_{\rm nt}$ peaks that follow HXR peaks whereas the loop top turbulent model would produce $V_{\rm nt}$ peaks that precede HXR peaks. The differences in $V_{\rm nt}$ behaviour in gradual and impulsive rise flares may suggest that different mechanisms for $V_{\rm nt}$ generation are dominant in the different classes. Turbulence at the loop top associated with the initial energy release (e.g. Tsuneta 1994, 1995) appears the dominant mechanism for $V_{\rm nt}$ generation in gradual rise flares because in these flares there is an overall tendency for the $V_{\rm nt}$ to peak before the HXR peak. Whereas for impulsive rise flares, the $V_{\rm nt}$ generally peaks after the HXR burst, hence the turbulent evaporation model appears more appropriate.

An alternative explanation for the different behaviour in gradual and impulsive rise flares, that may also explain the relationship between $t_{\rm rise}$ and $t_{\rm delay}$, may result from the inhomogeneity of the flare plasma. When calculating plasma parameters from the BCS spectrum we must assume the plasma is isothermal. However in both models there is a turbulent component (i.e. the evaporating plasma or the loop top plasma associated with the energy release) and a thermal component (i.e. stationary plasma in the flare loops), which may have different temperatures.

When the measured $V_{\rm nt}$ becomes dominated by emission from the thermal component it will begin to decrease, forming an observed peak. The time at which this occurs will depend on the evolution of the flare. For both the evaporation model and the loop top model the amount of turbulent plasma should correlate with the HXR flux with a positive or negative time lag. However the thermal component increases continually up to at least the end of the HXR burst. For flares that evolve slowly, i.e. those with a long HXR rise time ($t_{\rm rise}$), the thermal component can become stronger than the turbulent component early in the flare, hence the time delay between the $V_{\rm nt}$ and HXR peak ($t_{\rm delay}$) is also large. This effect can therefore describe the observed relationship between $t_{\rm rise}$ and $t_{\rm delay}$.

In summary, the different behaviour of $V_{\rm nt}$ in impulsive rise flare and gradual rise flares might imply that different mechanisms of $V_{\rm nt}$ generation are dominant or that the differences may arise as a result of a multi-thermal flare plasma and the corresponding difficulties of calculating the true value of $V_{\rm nt}$. With spatially resolved line profile observations, although we could not completely separate the evaporating plasma from stationary plasma or or loop top turbulent plasma we may be able to define regions where we expect either component to dominate. By comparing the temporal evolution of $V_{\rm nt}$ in these different areas to see if the peak times vary, we will be able to distinguish between non-isothermal effects and the presence of two $V_{\rm nt}$ generation mechanisms. In the simplest case if the peak times do vary this would indicate that

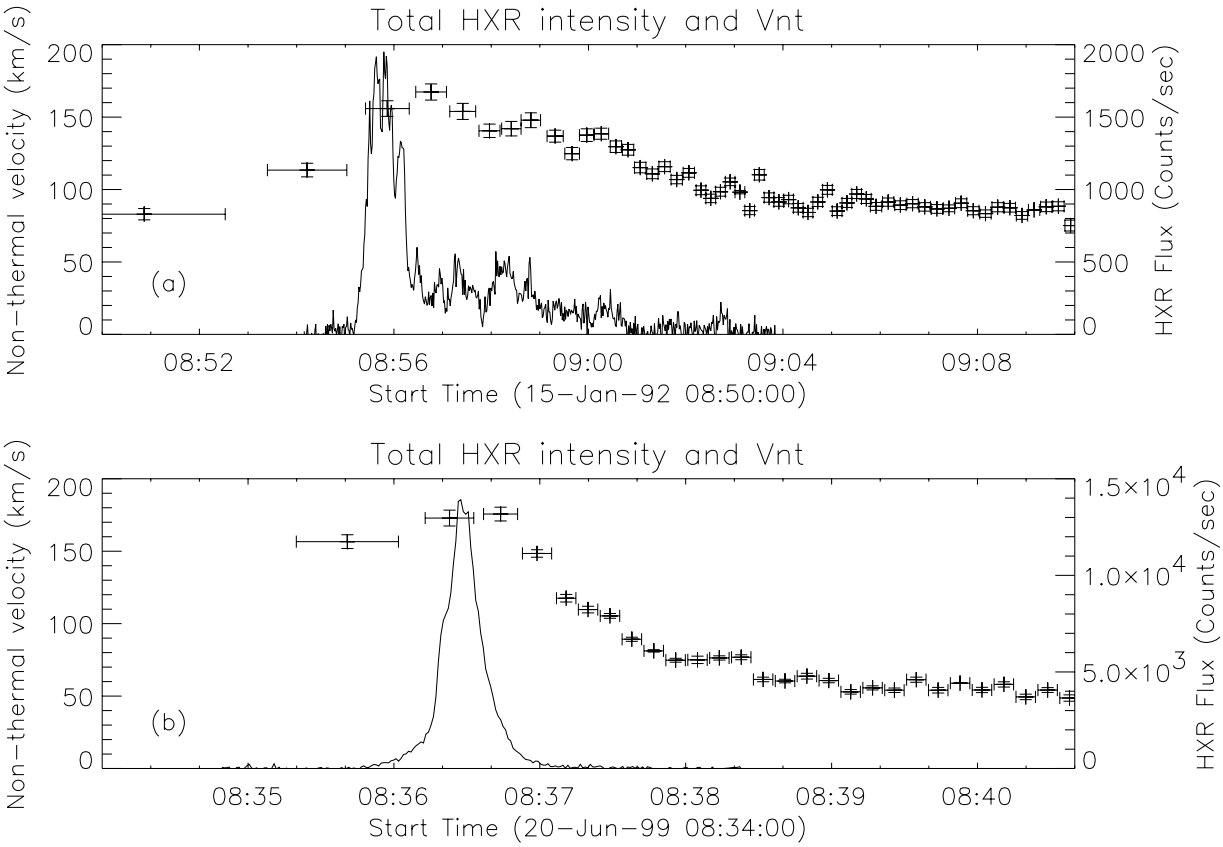

Fig. 5. Graphs showing $V_{\rm nt}$ (with error bars) and HXR flux. These are two examples that illustrate a possible relationship between the decay time of $V_{\rm nt}$ and the decay time of HXR flux. Note the time scales on each plot are not the same.

non-isothermal effects are strong. Spatially resolved line profile measurements will be available from the EUV imaging spectrometer (EIS) one of a suite of instruments to be launched on the Solar-B satellite in 2005.

References

Alexander, D., Harra-Murnion, L. K., Khan, J. I., & Matthews, S. A. 1998, ApJL, 494, 235
Bai, T., & Sturrock, P. A. 1989, ARA&A, 27, 421
Culhane, J. L., Hiei, E, Doschek, G. A., et al. 1991, Solar Phys., 136, 89
Fishman, G. J. 1989, Gamma-Ray Observatory Workshop, ed. W. N. Johnson (NASA/GSFC, Greenbelt, MD)
Khan, J. I., Harra-Murnion, L. K., Hudson, H. S., et al. 1995, ApJL, 452, 153
Mariska, J. T., & McTiernan, J. M. 1999, ApJ, 514, 484
Ranns, N. D. R., Matthews, S. A., Harra, L. K., & Culhane, J. L. 2000, A&A, 364, 859
Trow, M. W., Bento, A. C., & Smith, A. 1994, Nuclear Instruments and Methods in Physics Research, 348, 232
Tsuneta, S. 1994, X-ray Solar Physics from Yohkoh, ed. Y. Uchida, H. S. Hudson, T. Watanabe, & K. Shibata, 115
Tsuneta, S. 1995, Publ. of the Astronomical Society of Japan, 47, 691
Tsuneta, S. 1996, ApJ, 456, 840